Experimental Evaluation of Automatic Tuning of PID Controllers for an Electro-Mechanical System

Liuping Wang [*] **Chris Freeman** [**] **Eric Rogers** [**]

[*] *School of Engineering, RMIT University, Victoria 3000 Australia, (e-mail: liuping.wang@rmit.edu.au)*
[**] *Department of Electronics and Computer Science, University of Southampton, UK, (e-mail: {cf, etar}@ecs.soton.ac.uk)*

Abstract: Integrating processes are widely encountered in electro-mechanical systems and other areas. Automatic tuning of PID controllers for this type of system requires special consideration since the underlying system is unstable. Using relay feedback control in a closed-loop setting, an auto-tuner is designed to systematically find the controller parameters using a frequency sampling filter model. The performance of this auto-tuner is evaluated on an electro-mechanical experimental test facility that can be configured to operate in either as a single-input, single-output or multiple-input, multiple-output system. The experimental results demonstrate that when the interaction the between control loops is weak, the auto-tuner produces closed-loop performance that matches the specification, but this performance gradually decays as the level of interaction increases. The experimental results can also serve as experimental benchmarks to compare competing designs.

Keywords: Integrating systems, electro-mechanical systems, automatic tuning of PID controllers, experimental evaluation

1. INTRODUCTION

Automatic tuning of PID control has been of interest among control engineers over the past several decades, see, e.g., ((Astrom and Hagglund, 1984, 1988, 1995, 2006; Hang et al., 1991; Hagglund and Astrom, 1985; Yu, 2006; Johnson and Moradi, 2005)) for the reasons why PID controllers are the most widely used controllers in industrial applications. Auto-tuners must have the capability of setting parameters with minimal human intervention. A key component in all auto-tuners is the parameter estimation scheme designed to find the mathematical representation of a physical system. In previous work, (Hang et al., 1991) proposed the use of a set of pseudo-random-binary-sequence (PRBS) signals together with cross-correlation technique to identify the critical information needed for auto-tuner design. Alternatively, (Wang et al., 2001) proposed the use of the Fast Fourier Transform (FFT) to obtain the plant frequency response, the step response and a second-order model with time delay on which to base automatic tuning.

In other work, (Johnson and Moradi, 2005) and (Yu, 2006) introduced a range of PID controller design methods, including system identification using relay-feedback experiments and controller design methods. In (Lim et al., 2012) recursive least squares was used to estimate a discrete-time model to improve the closed-loop control performance of a sheet metal forming process and (Romero et al., 2011) developed an auto-tuning algorithm based on relay feedback control experiments by minimizing the load disturbance effects and maximizing the integral gain with minimum constraints on the gain and phase margins. Also (Yu Jin et al., 2014) extended the PID auto-tuning method to applications in the area of fractional systems with a time delay and (Dittmar et al., 2012) used of nonlinear optimization techniques to find the PID controller parameters in a multi-loop controller tuner. Finally, (Ho et al., 2000) extended the gain and phase margin design for PID control from single-input and single-output to multi-input and multi-output systems and (Cetin and Iplikci, 2015) developed an auto-tuner for nonlinear and multi-input multi-output systems.

The mechanism of relay feedback control, used by (Astrom and Hagglund, 1984), is widely regarded as the most effective instrument for auto-tuning and has been widely used in the design of auto-tuners. There are three key reasons for advocating the use of relay feedback control in the design of auto-tuners. The first is that relay feedback control will automatically generate an excitation input signal to ensure successful identification of process information that is relevant for the PID controller design. This is achieved without a priori information about the system dynamics, which is paramount in the design of an automatic tuning algorithm. The second is that the system is under closed-loop control with the nonlinear relay controller such that it is maintained at the operating condition chosen by the user. The third is that the sustained periodic oscillation generated by the relay feedback control produces an excellent signal-to-noise ratio for the estimation of critical process frequency information, which can be directly extracted using Describing Function Analysis ((Atherton, 1975; Astrom and Hagglund, 1984)), Fast Fourier Analysis (Wang et al., 2001) and frequency sampling filter based estimation (Wang and Cluett, 2000).

The majority of auto-tuners are designed for stable systems, e.g., chemical process control applications, where the processes are typically first order plus delay systems ((Hang et al.,

2002; Johnson and Moradi, 2005)). Recent years have seen increased interest in the control of electro-mechanical systems such as unmanned aerial vehicles ((Li and Song, 2012)) and autonomous underwater vehicles, e.g., (Bayat et.al, 2016). These systems have integrators in their underlying dynamics and the PID controllers are often used in their control, demanding the derivation of new auto-tuners to ensure high quality performance (Poksawat et al., 2016). Since integrating systems have pole on the stability boundary, stabilization is required before a relay experiment can be conducted.

This paper develops a new auto-tuner design with experimental evaluation on an electro-mechanical system. This new auto-tuner brings together several existing approaches in the areas of system identification and PID controller design for integrating systems.

2. AUTO-TUNER DESIGN FOR PID CONTROLLERS

This section describes the design of auto-tuner for PID control of integrating systems, which consists of four components: relay feedback control, recursive estimation of the frequency response, estimation of the integrating plus delay model and PID controller design. When the auto-tuner is applied to tune a cascade control system, the algorithm remains the same for both the inner and outer-loop controllers.

2.1 Relay Feedback Control

In the auto-tuner design, a proportional controller with known gain K_T is used to stabilize the integrating system and a relay feedback control system is applied to regulate the output. Figure 1 shows the configuration of the closed-loop system under relay feedback control. The reference signal $r(t)$ is a constant that represents the steady-state operation of the system output. Also ε is a hysteresis term selected to avoid possible random switches caused by the measurement noise and a is the relay amplitude. The signal $\bar{y}(t)$ represents the actual output measurement and the closed-loop control system is assumed to be in steady-state operation before the relay feedback control is switched on.

To ensure bumpless transfer, $r(t)$ is also used as the reference signal to the relay-feedback control loop. Assume that the relay feedback control is enabled at sampling instant t_0 and define the sampling interval as $\Delta t = t_k - t_{k-1}$. Also to initialize the relay element at the sampling time t_{-1}, $\bar{u}(t_{-1}) = r(t_{-1})$. For all $t_k \geq t_0$, the calculation of the reference signal for the closed-loop control system uses the following relay switching rules:

(1) Calculate the relay feedback error: $e(t_k) = r(t_k) - \bar{y}(t_k)$.
(2) If $|e(t_k)| \leq \varepsilon$; $\bar{u}(t_k) = \bar{u}(t_{k-1})$.
(3) If $|e(t_k)| > \varepsilon$; $\bar{u}(t_k) = r(t_k) + a \times sign(e(t_k))$.

This relay feedback control system will produce a sustained oscillation ((Atherton, 1975; Astrom and Hagglund, 1984)). Also if T is the period of the oscillation, it is well known that the frequency of the periodic signal $\bar{u}(t)$, denoted by $\omega_1 = \frac{2\pi}{T}$, has imaginary part approximately given by $-\frac{\pi\varepsilon}{4a}$.

2.2 Recursive Estimation of Frequency Response

To estimate the closed-loop frequency response

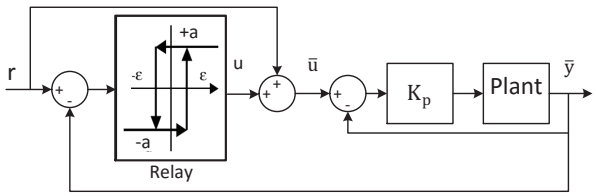

Fig. 1. Block diagram of the relay feedback control scheme.

$$T(j\omega_1) = \frac{K_T G(j\omega_1)}{1 + K_T G(j\omega_1)},$$

where $G(j\omega_1)$ is the open-loop frequency response at ω_1, the pair of input and output signals corresponding to the relay feedback control system is used, i.e., the input signal equals the relay output signal:

$$u(t) = \bar{u}(t) - r(t) = a \times sign(e(t)).$$

Also the closed-loop output signal with the steady-state removed is

$$y(t) = \bar{y}(t) - r(t) = -e(t).$$

A stable system with transfer-function $T(z)$ can, in general terms, be described in frequency sampling filter form as

$$T(z) = \sum_{l=-\frac{N-1}{2}}^{\frac{N-1}{2}} T(e^{jl\omega_d}) F^l(z), \tag{1}$$

where $\omega_d = \frac{2\pi}{N}$ denotes the fundamental frequency in discrete-time and $F^l(z)$ is the lth frequency sampling filter given by

$$\begin{aligned} F^l(z) &= \frac{1}{N} \frac{1 - z^{-N}}{1 - e^{jl\omega_d} z^{-1}} \\ &= \frac{1}{N}(1 + e^{jl\omega_d} z^{-1} + \ldots + e^{j(N-1)l\omega_d} z^{-(N-1)}). \end{aligned}$$

The output of the closed-loop control system under relay feedback with input $u(k)$ can be written as

$$y(k) = \sum_{l=-\frac{N-1}{2}}^{\frac{N-1}{2}} T(e^{jl\omega_d}) f^l(k) + v(k), \tag{2}$$

where $f^l(k)$ is the output of the lth frequency sampling filter and $v(k)$ is the output measurement noise, which is assumed to be Gaussian with zero mean and variance σ^2.

The magnitude of the filter output is inversely proportional to the parameter $|l|$ and additionally $|T(e^{jl\omega_d})|$ decreases as l increases. Hence in application the computational load is reduced by replacing (2) with an approximation constructed with a finite number of pairs of the frequency sampling filters and neglecting the remainder. In particular, the first three pairs are used, leading to

$$\begin{aligned} y(k) \approx\ & T(e^{j0}) f^0(k) + T(e^{j\omega_d}) f^1(k) + T(e^{-j\omega_d}) f^{-1}(k) + \ldots \\ & + T(e^{j3\omega_d}) f^3(k) + T(e^{-j3\omega_d}) f^{-3}(k) + v(k). \end{aligned} \tag{3}$$

Define the complex parameter vector to be estimated as

$$\theta = [T(e^{j0})\ T(e^{j\omega_d})\ T(e^{-j\omega_d})\ \ldots\ T(e^{j3\omega_d})\ T(e^{-j3\omega_d})]^*$$

and the corresponding regressor vector as

$$\phi(k) = [T(e^{j0})\ f^1(k)\ f^{-1}(k)\ \ldots\ f^3(k)\ f^{-3}(k)]^*$$

where * denotes the complex conjugate transpose. The frequency response parameters are estimated using a recursive least squares algorithm, i.e.,

$$\hat{\theta}(k) = \hat{\theta}(k-1) + P(k-1)\phi(k)\left(y(k) - \phi(k)^*\hat{\theta}(k-1)\right) \quad (4)$$

and

$$P(k) = P(k-1) - \frac{P(k-1)^*\phi(k)\phi(k)^*P(k-1)}{1+\phi(k)^*P(k-1)\phi(k)}, \quad (5)$$

where $\hat{\theta}(k)$ contains the estimated frequency response parameters.

2.3 Estimation of the Integrating Plus Delay Model

Given the proportional controller K_T, the frequency response of the plant $G(e^{j\omega_d})$ is calculated from the closed-loop frequency response relationship

$$T(e^{j\omega_d}) = \frac{G(e^{j\omega_d})K_T}{1+G(e^{j\omega_d})K_T}$$

and hence

$$G(e^{j\omega_d}) = \frac{1}{K_T}\frac{T(e^{j\omega_d})}{1-T(e^{j\omega_d})}. \quad (6)$$

Moreover, the discrete-time frequency response $G(e^{j\omega_d})$ closely approximates its continuous-time counterpart under the assumption that rapid sampling is employed and in such cases the equivalent continuous-time frequency is $\omega_1 = \frac{\omega_d}{\Delta t}$. Letting $G_p(j\omega_1)$ denote the plant continuous-time frequency response at the fundamental frequency ω_1, it follows that

$$G_p(j\omega_1) \approx G(e^{j\omega_d}).$$

For an integrating plus time delay system, a single frequency is sufficient to determine its gain K_p and time delay d. The approximate model of an integrating system is assumed to take the form:

$$G_p(s) = \frac{K_p e^{-ds}}{s}. \quad (7)$$

Also letting the frequency response of the integrator plus delay model (7) be equal to the estimated $G_p(j\omega_1)$ gives

$$\frac{K_p e^{-jd\omega_1}}{j\omega_1} = G_p(j\omega_1) \quad (8)$$

and equating the magnitudes on both sides of (8) gives

$$K_p = \omega_1|G_p(j\omega_1)|, \quad (9)$$

where $|e^{-jd\omega_1}| = 1$. Also, from (8)

$$e^{-jd\omega_1} = \frac{j\omega_1 G_p(j\omega_1)}{K_p}$$

and hence an estimate of the time delay is

$$d = -\frac{1}{\omega_1}tan^{-1}\frac{Imag(jG_p(j\omega_1))}{Real(jG_p(j\omega_1))}. \quad (10)$$

Once the integrator plus time delay model is obtained, the PID controller parameters are calculated using the tuning rules given in (Wang and Cluett, 1997) and (Wang and Cluett, 2000). Although there are many design methods available for an integrator plus time delay model, e.g. (Tyreus and Luyben, 1992), the set of tuning rules adopted here has the characteristics of being simple and robust and were developed using frequency response analysis without approximation of the time delay. Using these tuning rules, the PID controller parameters are calculated using the normalized parameters:

$$K_c = \frac{\hat{K}_c}{dK_p}; \tau_I = d\hat{\tau}_I; \tau_D = d\hat{\tau}_D$$

For a damping coefficient $\xi = 1$, the normalized PID controller parameters are calculated using

$$\hat{K}_c = \frac{1}{0.5080\beta + 0.6208}, \quad (11)$$

$$\hat{\tau}_I = 1.9885\beta + 1.2235, \quad (12)$$

$$\hat{\tau}_D = \frac{1}{1.0043\beta + 1.8194}, \quad (13)$$

where the parameter β is the scaling factor for the desired closed-loop time constant, i.e.,

$$\tau_{cl} = \beta d$$

For a larger β, a larger desired closed-loop time constant is selected, implying a slower closed-loop response speed for disturbance rejection and reference following. An advantage of the tuning rules is that the selection of β gives both the desired closed-loop time constant and the gain and phase margins for the closed-loop system ((Wang and Cluett, 2000)). For example, when $\beta = 2$, the gain and phase margins for a PID control system are approximately 3° and 45°, whereas for a PI control system they are approximately 2° and 40°.

3. EXPERIMENTAL SYSTEM

This section gives the results and associated discussion of applying the auto-tuners to a two-input two-output electro-mechanical platform whose design and commissioning is detailed in (Freeman and Dinh, 2014; Dinh et al., 2014). This system employs differential gearboxes connected via spring-mass-damper systems, and driven by both induction and DC motors. In these tests it is configured as a two input, two output layout as shown in Figure 2 where I, B and K denote inertial, damping and stiffness parameters respectively. The

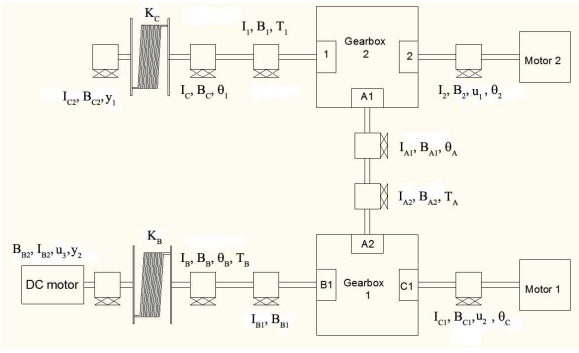

Fig. 2. System configuration showing placement of disturbance injection.

inputs to the system are voltage demand signals fed to the induction motors $\{u_1, u_2\}$ and the outputs are the angular displacements (radians) of the spring-mass-damper sections $\{y_1, y_2\}$. Note that this is only one possible configuration of inputs and outputs, since the position and number of motors can be easily altered without changing the central structure.

This configuration has a level of interaction which can be manipulated using the lumped damping parameter $B_{A1} + B_{A2}$.

Injection of noise and disturbance can be realized mechanically using the DC motor, but this is not employed in the current test procedure. The system transfer-function model is

$$\begin{bmatrix} y_1(s) \\ y_2(s) \end{bmatrix} = \begin{bmatrix} G_{11}(s) & G_{12}(s) \\ G_{21}(s) & G_{22}(s) \end{bmatrix} \begin{bmatrix} u_1(s) \\ u_2(s) \end{bmatrix}. \quad (14)$$

The differential gears are custom-made to eliminate backlash and reduce inertia and friction, and gearing between devices is implemented via belt drives to reduce the overall footprint and ensure low backlash. The damping parameter $B_{A1} + B_{A2}$ is realized using four adjustable dampers geared together, and the level of interaction is parameterized by c which varies between 0 (no interaction, maximum damping), and 1 (full interaction, minimum damping). The final implementation of the two input, two output system is shown in Figure 3.

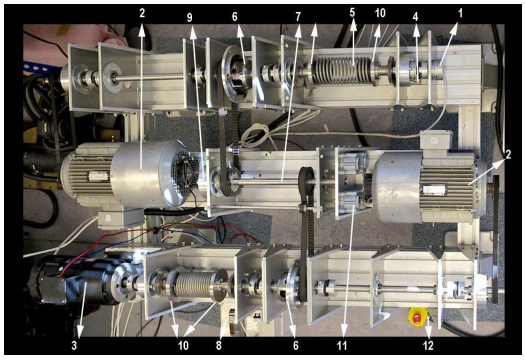

Fig. 3. MIMO system components: 1) encoder, 2) induction motors, 3) DC motor, 4) rotary damper, 5) torsional spring, 6) differential gearboxes, 7) coupling shaft, 8) DC motor controller, 9) clamp, 10) inertia, 11) adjustable interaction dampers, 12) emergency stop button.

The two induction motors are equipped with integrated 2000 pulse per revolution encoders, and the outputs are fitted with 2500 pulse per revolution encoders. Each 1.1 kW AC induction motor is connected to an inverter configured in velocity mode, and the 1.5 kW DC motor uses a four quadrant drive. Real-time hardware comprises a ds1103 dSpace board which interfaces directly with Matlab/Simulink to enable rapid controller development and implementation at 1000 Hz.

4. EXPERIMENTAL RESULTS

The electro-mechanical system has integrators since the outputs are the angular positions of spring-mass-damper sections. The system model had been identified experimentally where sinewaves of different frequency and amplitude have been injected into the inputs, and transfer-functions have been fitted to the resulting Bode plots, using the Least Mean Squares (LMS) approach (Dinh et al., 2014). The transfer-function entries are of high order with integrators (see (Dinh et al., 2014)). Instead of using the transfer-function models, the results in this section were obtained by directly applying the auto-tuner to determine the PID controllers. Three different levels of interactions are used through changing the configurations of the system. When the parameter $c = 0$, the electro-mechanical system is configured as two independent single-input single-output systems. When $c = 0.4$, there is moderate interaction, and strong interaction when $c = 0.8$. The auto-tuning procedure remains the same for all tests with the same amplitude ($a = 1.75$) and the same hysteresis ($\varepsilon = 0.9$), however, the proportional gain K_T is different in each case.

In the automatic tuning process, the relay feedback control is first applied to the input-output pair (u_1, y_1) using K_T, $a = 1.75$ and $\varepsilon = 0.9$ where the input signal u_2 is set equal to 0. Given the relay feedback experimental data, the PID controller parameters are identified for the input-output pair (u_1, y_1). Then this tuning procedure is repeated for the input-output pair (u_2, y_2) with the same relay amplitude and hysteresis but a different proportional gain K_T. With the corresponding relay-feedback control experimental data, the PID controller parameters are identified for the input-output pair (u_2, y_2). Figure 4 shows the input and output data for the pair (u_1, y_1) under the relay feedback control. It is seen that as c increases, the effects of output y_2 on the relay control signal u_1 increases. Additionally, the amplitude of y_2 increases even when the input signal u_2 is set to be zero. Parallel experimental results were produced for the pair (u_2, y_2) and are shown in Figure 5.

Table 1 shows the K_T parameters and the resulting PID controller parameters obtained from applying the auto-tuner. The two feedback PID controllers are then simultaneously applied using input-output pairs (u_1, y_1) and (u_2, y_2). During testing, a unit step was selected as the reference for each output channel. Figure 6 shows the inputs and outputs of the MIMO system for the three cases of interaction.

The last column of Table 1 shows the mean squared error for each output using the three cases of interaction. The mean squared error is defined as $\frac{1}{M}\sum_1^M e(t_i)^2$, where M is the number of samples and $e(t_i)$ is the error between the reference and output signal with the PID controller operating.

Case	K_T	K_c	τ_I	τ_D	$\frac{1}{M}\sum_1^M e(t_i)^2$
$c = 0$ u_1, y_1	0.3	0.476	0.588	0.092	0.018
$c = 0$ u_2, y_2	0.12	0.243	0.602	0.095	0.019
$c = 0.4$ u_1, y_1	0.25	0.518	0.572	0.090	0.019
$c = 0.4$ u_2, y_2	0.2	0.321	0.634	0.099	0.019
$c = 0.8$ u_1, y_1	0.2	0.483	0.476	0.075	0.033
$c = 0.8$ u_2, y_2	0.2	0.362	0.639	0.100	0.021

Table 1. PID controller parameters for different c values.

5. CONCLUSIONS

This paper has considered the design and application of auto-tuners to integrating processes. This has exploited relay control and frequency sampling filters. A major part of the results reported are from experimental application of a two-input two-output electro-mechanical system where the level of interaction in the channels can be varied. The results show that the auto-tuning design is capable of producing high quality performance but this lessens as the interaction increases. These results serve as a basis for future research both on the design algorithms themselves but, equally importantly, as a set of experimental benchmarks that can be compared with other designs. Also it is possible to inject noise and the performance of the auto-tuner in this case should be investigated.

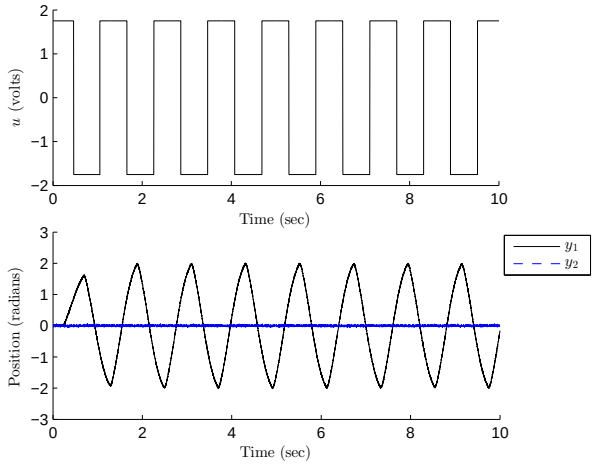

(a) $c = 0$

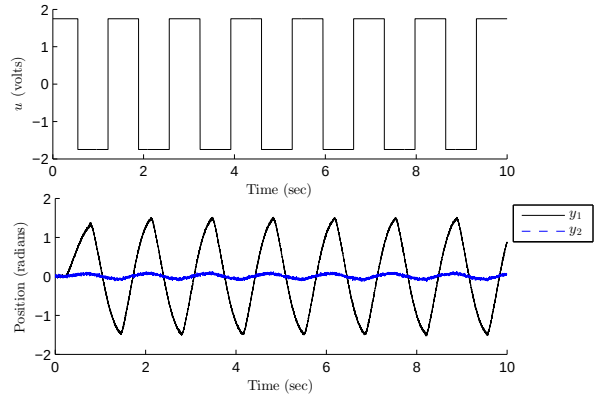

(b) $c = 0.4$

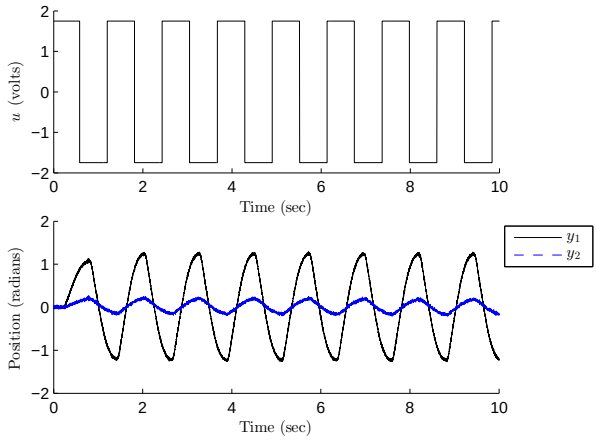

(c) $c = 0.8$

Fig. 4. Input and output data from the relay control for (u_1, y_1)

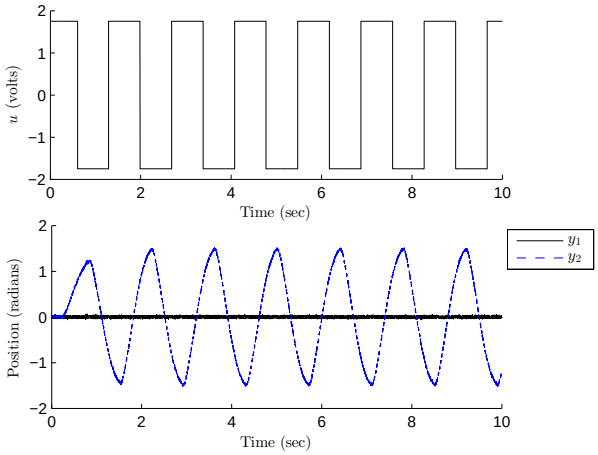

(a) $c = 0$

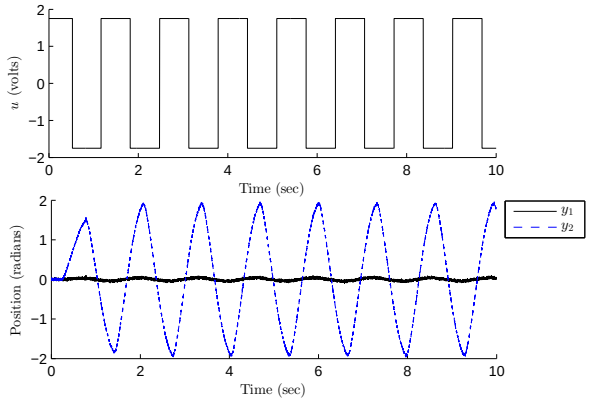

(b) $c = 0.4$

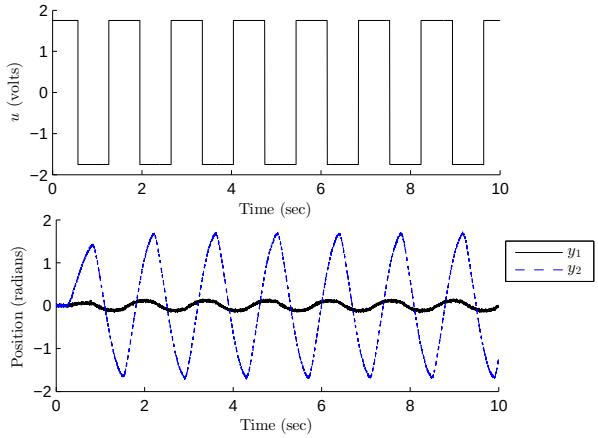

(c) $c = 0.8$

Fig. 5. Input and output data from the relay control for (u_2, y_2)

REFERENCES

Astrom, K.J. and Hagglund, T. (1984). Automatic tuning of simple regulators with specifications on phase and amplitude margins. *Automatica*, Vol.20, 645–651.

Astrom, K.J. and Hagglund, T. (1988). *Automatic Tuning of PID Controllers*. Instrument Society of America, Research Triangle Park, NC.

Astrom, K.J. and Hagglund, T. (1995). *PID Controllers:Theory, Design, and Tuning*. Instrument Society of America, Research Triangle Park, NC.

Astrom, K.J. and Hagglund, T. (2006). *Advanced PID control*. Instrument Soc. of America, Research Triangle Park, NC.

Atherton, D.P. (1975). *Nonlinear Control Engineering-Describing Function Analysis and Design*. Van Nostrand Reinhold Co., London, UK.

Cetin, M. and Iplikci, S. (2015). A novel auto-tuning PID control mechanism for nonlinear systems. *ISA transactions*, 58, 292–308.

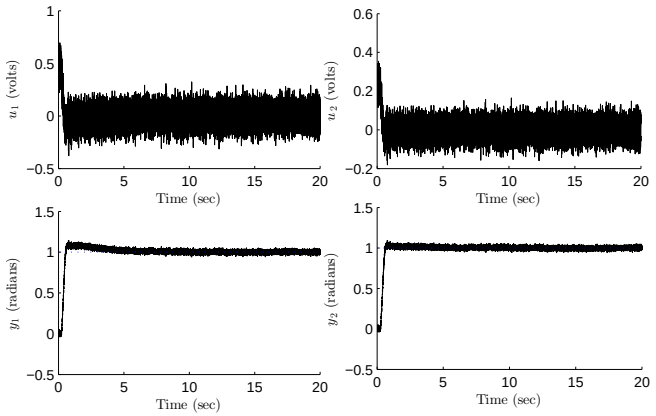

(a) $c = 0$

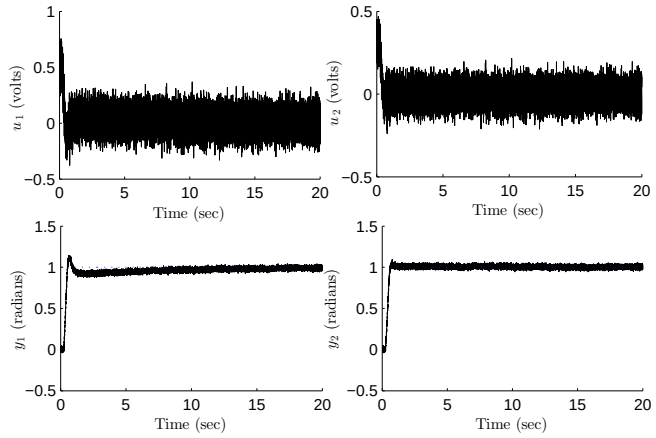

(b) $c = 0.4$

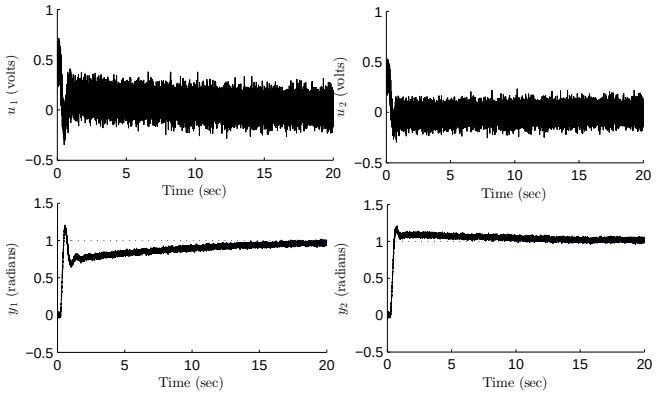

(c) $c = 0.8$

Fig. 6. Closed-loop PID control results

Dinh, T.V., Freeman, C.T., and Lewin, P.L. (2014). Assessment of gradient-based iterative learning controllers using a multivariable test facility with varying interaction. *Control Engineering Practice*, 29, 158–173.

Dittmar, R., Gill, S., Singh, H., and Darby, M. (2012). Robust optimization-based multi-loop PID controller tuning: A new tool and its industrial application. *Control Engineering Practice*, 20(4), 355–370.

Freeman, C.T. and Dinh, T.V. (2014). Experimentally verified point-to-point iterative learning control for highly coupled systems. *International Journal of Adaptive Control and Signal Processing*, 89(3), 302–324.

Hagglund, T. and Astrom, K.J. (1985). Method and an apparatus in tuning a PID-regulator. *United States Patent*, 4549123.

Hang, C.C., Astrom, K.J., and Ho, W.K. (1991). Refinements of the Ziegler-Nichols tuning formula. *IEE Proceedings, PtD*, 138, 111–118.

Hang, C. C., Astrom, K.J., and Wang, Q. G. (2002). Relay feedback auto-tuning of proces controllers- a tutorial review. *Journal of Process Control*, 12, 143–162.

Ho, W., Lee, T., and Xu, W. (2000). The direct Nyquist array design of PID controllers. *IEEE Transactions on Industrial Electronics*, 47(1), 175–185.

Johnson, M.A. and Moradi, M.H. (2005). *PID Control: New identification and design methods*. Springer Verlag, New York, USA.

Li, Y. and Song, S. (2012). A survey of control algorithms for quadrotor unmanned helicopter. *2012 IEEE 5th International Conference on Advanced Computational Intelligence, ICACI 2012*, 365–369.

Lim, Y., Venugopal, R., and Galip Ulsoy, A. (2012). Auto-tuning and adaptive control of sheet metal forming. *Control Engineering Practice*, 20(2), 156–164.

Poksawat, P., Wang, L., and Mohamed, A. (2016). Automatic tuning of attitude control system for fixed-wing micro aerial vehicles. *IET Proceedings on Control Theory and Applications*, 10, 2233-2242.

Bayat, M., Crasta, A., Aguir, A. P. and Pascoal, A. (2016). Range-based underwater vehicle localization in the presence of unknown ocean currents: theory and experiments. *I*EEE Trans. Control Systems Technology, 24(1), 123–139.

Romero, J.A., Sanchis, R., and Balaguer, P. (2011). PI and PID auto-tuning procedure based on simplified single parameter optimization. *Journal of Process Control*, 21(6), 840–851.

Tyreus, B.D. and Luyben, W.L. (1992). Tuning PI controllers for integrator/dead time processes. *Industrial & Engineering Chemistry Research*, Vol.31, 2625–2628.

Wang, L. and Cluett, W.R. (1997). Tuning PID controllers for integrating processes. *IEE Proceedings on Control Theory and Applications*, Vol. 142, 385–392.

Wang, L. and Cluett, W.R. (2000). *From Plant Data to Process Control: Ideas for Process Identification and PID Design*. Taylor and Francis, London.

Wang, Q.G., Zhang, Y., and Guo, X. (2001). Robust closed-loop identification with application to auto-tuning. *Journal of Process Control*, 11, 519–530.

Yu, C.C. (2006). *Autotuning of PID controllers.* Springer Science & Business Media.

Yu Jin, C., Ryu, K.H., Sung, S.W., Lee, J., and Lee, I.B. (2014). PID auto-tuning using new model reduction method and explicit PID tuning rule for a fractional order plus time delay model. *Journal of Process Control*, 24(1), 113–128.